# Spring wheat biomass estimation by proximal and remote methods in condition of academical field of central Russia

*Nikita* Aleksandrov[1*], *Maria* Bobrovskaya[1], *Ivan* Seregin[1], and *Alexey* Buzylev[1]

[1] Russian State Agrarian University—Moscow Timiryazev Agricultural Academy, Ecology Department, Timiryazevskaya Street 49, Moscow, Russia

**Abstract.** The paper presents the results of comparison of remote and proximal methods of spring wheat biomass monitoring. The study showed a linear relationship between data obtained with groups of methods at early stages of plant development (tillering, booting), when at later stages (earing, flowering) - the methods showed different degrees of interchangeability and did not have a clear relationship between them.

## 1 Introduction

Remote sensing has become a routine practice in agriculture in recent years. Satellite information allows to solve such typical tasks as providing current control over the state of crops; preliminary forecasting of crop yields; monitoring of harvesting rates over vast territories; capacity of different pastures and productivity of grasslands. In general, all the above makes it possible to realize effective support for management decisions in agriculture [1].

Remote sensing applications in agriculture are generally categorized according to the type of sensor platforms: satellite (remote sensing), unmanned (aerial) and ground-based (proximal). These platforms and their associated imaging systems can be differentiated by the height of the platform, image spatial resolution, and minimum data acquisition frequency. As spatial resolution increases, the area of the smallest pixel decreases and the uniformity of soil or crop characteristics within that pixel increases [1].

In agriculture, satellites have been used for imaging since 1972 [2,3], when Landsat 1 (originally known as Earth Resources Technology Satellite 1) was launched. The multispectral scanning system (MSS) on Landsat 1 was capable of imaging in the green, red, and two infrared bands with a spatial resolution of 80 m, with a data acquisition frequency of 18 days. Landsat 1 was initially used to determine agricultural landscapes occupied by corn and soybean crops (USA) with an overall accuracy of 83% [2].

One of the key elements of agroecological optimization of modern technologies of grain crops cultivation is field methods of agroecological monitoring, in which digital technologies of operational processing of data on the state of crops obtained using unmanned aerial vehicles (UAV) are increasingly actively introduced [3].

Based on the data obtained from the UAVs it is possible to estimate the workload of agricultural operations and control their implementation, predict the phenology of grain crops, fertilizer application optimization and optimal dates for harvesting [4]

Remote sensing data obtained using UAVs have higher spatial and temporal resolution compared to satellite images, and compared to conventional aircraft UAVs have lower cost, weight, and potentially higher resolution due to lower minimum altitude and flight speed [3]. Another advantage of UAVs is the possibility to obtain a digital elevation model with very high resolution along with orthophoto. This allows both to obtain georeferencing of high enough resolution for soil parameters mapping [5] and extrapolate the data of soil parameters point measurements to produce high resolution mapping [6].

At the same time, most crop models are still based on satellite data, while UAV data, although used quite successfully for yield prediction, are still analyzed only in a few papers [7]. Therefore, we decided to test how detailed information including biomass parameters such as crop height, projective cover and LAI can be predicted with cheap and widespread UAV model on different phenological phases.

## 2 Material and method

The experiment was organized in 2023 on the experimental fields of K.A. Timiryazev Russian State Agricultural University-MSHA on the north of Moscow.

The relief of the site is represented by a plain with weakly expressed microrelief. Absolute heights of the field area are in the range of 166-170 meters. Along the boundaries of the site there is a drainage channel (Fig. 1).

*Correspondence author: Alexandrov_na@rgau-msha.ru

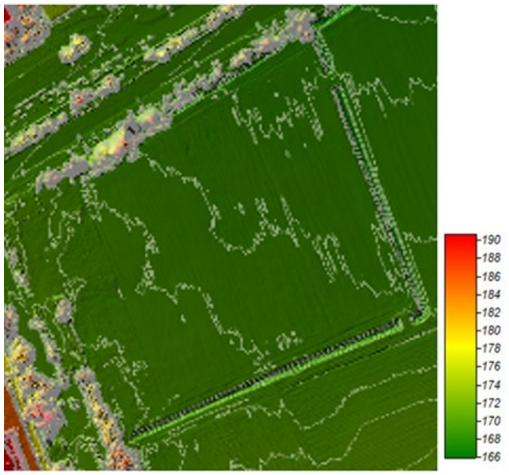


**Fig. 1.** Terrain map of experimental field.

The experimental field was divided into 81 quadrats, coded from A-1 to I-9, with one sampling point inside each quadrat, as shown in Fig. 2, all measurement inside quadrant was done threefold.

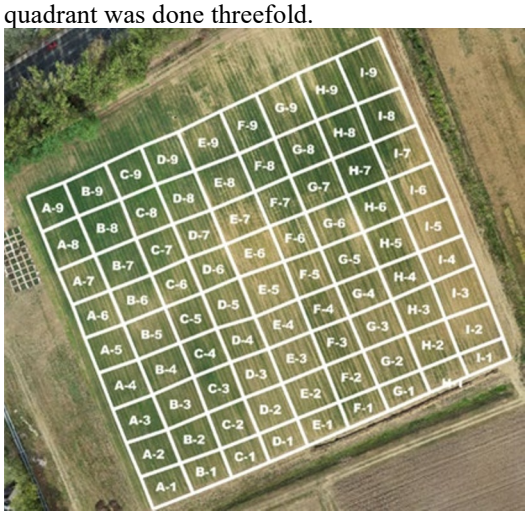

**Fig. 2.** Field sampling scheme.

Plant height was measured using a measuring tape at the tillering and booting phases, the height was measured from the soil surface to the top leaf. Starting from the earing phase - from the soil surface to the top of the ear, the length of the ear was considered separately. The projective coverage was calculated using a digital RGB camera with a resolution of 50 megapixels and a shooting height of 1.5 meters above the ground. The photo was taken in such a way that the picture included a wire frame on the ground surface with dimensions of 0.5x0.5 meters. Georeferencing of the RGB images was recorded using GPS data extracted from mobile devices. The coordinates were further used to calculate the projective coverage for each quadrant.

The obtained images were cropped along the boundaries of the wire frame and processed in the ImageJ software [8]. The image was converted from RGB color space into Hue, Saturation, Brightness (HSB) one. Using the "color threshold" tool, the green range was selected on the color gradient so that the entire surface of plant leaves was selected on the image. Then the image was adjusted using brightness and saturation parameters. This adjustment allows to exclude elements in the image that do not belong to vegetation. Using the "analyze" and "measure" tools, the program calculated the "area" parameter - the area of all extracted pixels. Then this value was recalculated by the number of pixels in the image and converted into percentages.

During the period from 16.06.2022 to 29.08.2022 weekly in the morning, the area was filmed with a DJI Phantom-4 RTK drone equipped with a camera with a 1 inch CMOS sensor, the images were obtained with a resolution of 20 megapixels. Shooting was performed in RGB mode, and the shooting altitude was 70 m. The longitudinal and transverse overlap of imaging was 80%.

The obtained RGB images were processed using Agisoft Metashape, where photogrammetric processing of digital images was performed, resulting in orthophotos of the fields with spatial resolution of 2.5cm and a digital elevation model for each flight date.

Using the obtained orthophotos, the projective coverage was calculated in the QGIS program. Vegetation indices were calculated for each orthophoto using the QGIS raster calculator according to the formulas in Table 1 [8]. At the next stage, from all resulting raster files with values of indices for different dates, 81 fragments corresponding to the boundaries of experimental squares were cut out using vector masks.

**Table 1.** Vegetation indices.

| **Vegetation Index (VI)** | **Formulae** |
|---|---|
| Normalized Difference Yellowness Index | NDYI = (G-B)/(G+B)) |
| Normalized Green Red Difference Index | NGRDI = (G - R)/(G + R) |
| Triangular Green Index | TGI = -0.5*(190*(r-g)-120*(r-b)) |
| Visible Atmospherically Resistant Index | VARI = (G - R)/(G + R - B) |
| Green Leaf Index | GLI = (2*G - R - B)/(2*G + R + B) |
| Modified Photochemical Reflectance Index | MPRI = (G-R)/(G+R) |
| Red Green Blue Vegetation Index | RGVBI = (g - b*r)/(g*g+r*b) |
| Modified Green Red Vegetation Index | MGVRI = (g*g-r*r)/(g*g+r*r) |
| Excess Green Red Vegetation Index | ExGR = ExG - ExR |
| Excess Red Vegetation Index | ExR = (1.4*r - g) |
| Excess Green Vegetation Index | ExG = (2*g-r-b) |
| Vegetativen Index | VEG = g/(r^0.667*b^0.333) |
| Normalized Red | r = R/(R+G+B) |
| Normalize Green | g = G/(R+G+B) |
| Normalized Blue | b = B/(R+G+B) |

LAI was measured using a LICOR LAI-2200C and an AccuPAR LP-80 ceptometer. Biomass and yield were measured by direct harvests on a 0.25 by 0.25 m square plots.

## 3 Results and discussion

The projective coverage was calculated using both UAV remote sensing data and proximal data from crop surveys at the sites. Comparison of these data by phenophases showed that the maximum and statistically significant correlation between the indicators of projective cover calculated according to the two methods is reached in the tillering phase $R^2$=0,48 Relatively low values of linear relationship at later stages are associated with an increase in spatial heterogeneity of biomass distribution in the field, due to the large heterogeneity of soil cover. Thus, already at the earing phase the strength of linear relationship between projective cover measured by two methods decreased $R^2$=0.18.

Fig. 7a and 7b show correlograms of dependencies of individual biomass parameters and vegetation indices measured by proximal and remote methods at the time of tillering and booting phases, respectively. The scale of Pearson correlation coefficient values is presented on the right side of the figure. Only statistically significant dependencies, p<0.01, are presented on the graph.

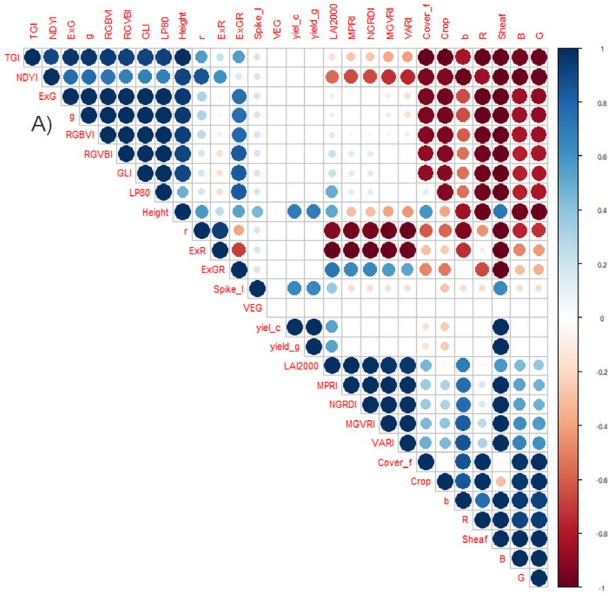


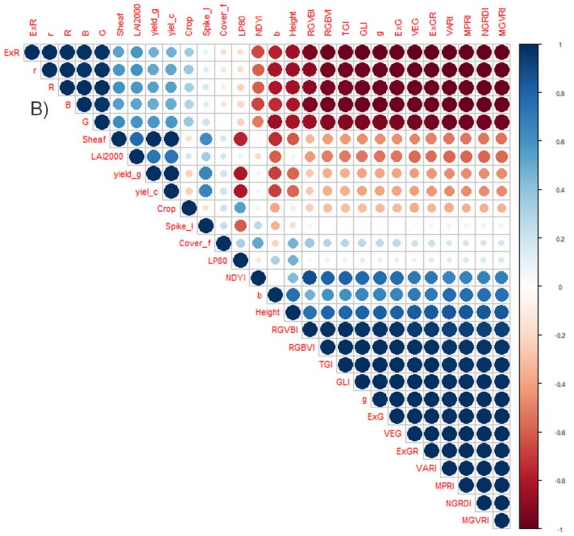


**Fig. 7.** Correlogram of dependencies of individual biomass parameters and indices measured by proximal and remote methods at the phase of tillering A) and booting B).

The data obtained by LI-COR LAI2200C were used to estimate the LAI biomass parameter, since the instrument is considered the standard for determining this index in the academic environment. According to the correlation analysis data, the highest correlation coefficient is observed in the relationship between the LAI parameter and indices, namely ExGR, ExR, r, MPRI, NGRDI, MGVRI, VARI, b, where |r|≥ 0.7. Hence, these indices can be utilized to predict LAI. The projective coverage has weak predictive power.

The highest correlation coefficient is observed in the relationship between the height parameter and the indices: R, G, B, g, b, RGBVI, RGVBI, GIL, TGI, ExG and NDYI, where |r|≥ 0.7. Hence, these indices can be applied to predict plant heights. The projective coverage has an average predictive power comparable to the LP-80 data. At tillering stage, the LAI2200C is not recommended for wheat growth prediction.

It is best to use Lp-80 for yield prediction because the correlation coefficient is -0.8. Using the height parameter for prediction is also applicable as r = 0.7. The LAI2200C instrument gave a weak correlation with yield. Indices and projective cover gave no relationship and are not recommended for yield prediction at tillering stage.

Analysis of the relationship between the variables yield and LAI index measured by LAI-2200C proximal sensor at the stage of tube emergence showed a strong relationship, as the correlation coefficient is equal to 0.7. TheLP-80 instrument has a weaker relationship r = - 0.4. The vegetation indices have correlation coefficient |r|≤ 0.6, except for the b index, which showed the strength of relationship comparable to LAI2200C (Fig.7B).

At the booting phase, the LAI parameter is generally predicted weaker than at the tillering stage. The highest correlation coefficient |r| = 0.6 characterizes the relationship with indices R, G, r, b, RGVBI, MGVRI, VARI, NGRDI, TGI, ExGR, VEG. The indices B, g, RGBVI, GIL, and ExR have the lowest predictive power |r| = 0.5. Projective coverage is not recommended because the correlation coefficient is 0.2.

At later stages all correlation between proximaly and remotely sensed biomass parameters dropped dramatically, and only few pairs had statistically significant relation.

## 4 Conclusion

Based on the summary data for predicting height, leaf area index and yield of wheat, the remote method using a cheap RGB camera gives results comparable to proximal methods using sophisticated tools. At the same time, proximal and remote methods are compatible at most phenological phases, especially at early stages (tillering - booting).

## Funding

The research was financed by the Ministry of Science and Higher Education of Russian Federation, Agreement No. 075-15-2021-1030.

## References

1. J. Liu et al., Remote sensing of environment, T. 62, №. 2, 158-175 (1997)
2. W. Lafayette, IN: Purdue Univ. P.C. Doraiswamy, S. Moulin, P.W. Cook, A. Stern Photogrammetric Engineering & Remote Sensing, **69**, 6, 665-674 (2003)
3. C.J. Strong, N.G. Burnside, D. Llewellyn, PloS T., **12**, 10, C. e0186193 (2017)
4. A. Buzylev, M. Tihonova, E. Taller, I. Vasenev. *Agroecological modeling of spring barley cultivation technology in the conditions of the Penza region.* In BIO Web of Conferences, 37, p. 00065 EDP Sciences (2021)
5. V.P. Samsonova, J.L. Meshalkina, Blagoveschensky, et.al, Precision Agriculture, **19**, 1085-1099 (2018)
6. Y. Dvornikov, M. Slukovskaya, A. Yaroslavtsev, et al., Land Degradation & Development, **33**, 1731-1744 (2022)
7. A.I. de Castro, Y. Shi, J.M. Maja, J.M. Peña, Remote Sensing, **13**, 11, 2139 (2021)
8. P.J. Zarco-Tejada, et al., IEEE Transactions on Geoscience and Remote Sensing, **39**, 7, 1491-1507 (2001)